ISSN: 2414-1895 DOI: 10.6919/ICJE.202303_9(3).0008

# Dynamic Characteristics Analysis of Aluminum Foam Anti-collision Pier under Vehicle Impact

Yuxi Yan

School of Civil Engineering, Henan Polytechnic University, Jiaozuo 454000, China

m18739127710@163.com

## Abstract

**To study the influence of aluminum foam anti-collision device on dynamic characteristics of bridge pier under vehicle impact. Using ANSYS/LS-DYNA software, the finite element models of piers with and without aluminum foam anti-collision devices were established respectively, and the dynamic characteristics of piers were calculated and analyzed under the two conditions. The impact force, pier displacement, pier stress and vehicle acceleration were compared in the two cases, and combined with the energy conversion results, the protection effect of aluminum foam anti-collision device on vehicles and piers was analyzed. The results show that when there is aluminum foam anti-collision device, most of the kinetic energy of the vehicle is absorbed by the anti-collision device, and the impact force, pier displacement, pier stress and vehicle acceleration of the vehicle on the pier are significantly reduced. The aluminum foam anti-collision device can effectively protect the vehicle and pier.**

## Keywords

**Vehicle-bridge Collision; Collision Dynamic Characteristics; Foamed Aluminium; Collision-Prevention Device.**

## 1. Introduction

China has a large land area, and its population and cities are scattered from east to west. By the end of 2011, the total length of highways in China had reached 4.106 million kilometers, and the planned total size of the national highway network was 401,000 kilometers. The construction of highway network can greatly improve the convenience of the city, but limited to various conditions, there are many Bridges, and Bridges located at the intersection of traffic routes. So there will be a risk of being hit by passing vehicles. In recent years, with the increase of the traffic volume, the accident of vehicle collision with the bridge also occurs constantly, causing loss of life and property, vehicle damage and pier damage or even collapse. Dong Zhengfang et al. [1] made classified statistics on 502 bridge collapse accidents in 66 countries in the world. There were 19 bridge collapse accidents caused by vehicle impact, accounting for the eighth place in the total number of bridge collapses. Therefore, it is of great application value to deeply study the dynamic characteristics of bridge pier and design a reasonable and effective anti-collision device.

Vehicle impact test is difficult and costly, and the research results of part of impact impact test [2-4] show that it is reliable to apply numerical simulation method to vehicle-bridge impact problem, and numerical simulation has become an important and effective method to study collision problems. Zeng Xiangguo et al. [5] adopted the Chevy Truck model released by NCAC (National Crash Analysis Center) of the United States to conduct numerical simulation on the vehicle impact pier, analyzed the dynamic response of the pier under different impact speeds, and calculated four vehicle impact force evaluation indexes. It is also compared with three bridge design codes in America,

ISSN: 2414-1895 DOI: 10.6919/ICJE.202303_9(3).0008

Europe and China. In order to reduce the consequences of vehicle collision with pier, many scholars study the anti-collision effect of different anti-collision devices to reduce the damage. Han Yan et al. [6] conducted a model test on the dynamic performance of the outsourced steel plate concrete pier under vehicle collision, and concluded that the outsourcing steel plate method can effectively reduce the impact of vehicles on the pier. Wang Junjie et al. [7] proposed a practical steel plate-rubber ring anti-collision device through numerical simulation and statistical analysis, and gave relevant design examples according to the design process. Aluminum foam is a new structural and functional material with both metal and foam characteristics. It is made by adding additive foam into pure aluminum or aluminum alloy [8]. Aluminum foam material has the characteristics of light weight, good energy absorption. when the impact force is small, aluminum foam material can absorb a lot of energy through elastic and plastic deformation, so it is suitable for engineering structure protection.

Based on a bridge pier as a prototype, this paper establishes a bridge pier model of vehicle impact on bare pier and impact with aluminum foam anti-collision device by ANSYS/LS-DYNA, and compares and analyzes the dynamic characteristics of energy conversion, impact force, pier top displacement, pier impact surface stress and vehicle acceleration under the two conditions, so as to study the anti-collision effect of aluminum foam anti-collision device. It provides the basis for the research and design of bridge pier anti-collision.

## 2. Finite Element Model of Vehicle-pier Impact

### 2.1 Pier Model

The reinforced concrete pier of a bridge is taken as the prototype, which is a solid cylindrical pier. The main dimensions and reinforcement are shown in Figure 1. The height of the pier is 8.5m and the diameter is 1.5m. 24 longitudinal reinforcement bars are uniformly arranged along the circumference of the pier, and HRB335 ribbed bars with a diameter of 25mm are adopted. The stirrup adopts HPB235 smooth steel bar with diameter of 10mm and spacing of 20cm. The protective layer of reinforcement is 50mm thick, and the pier is made of C40 concrete.

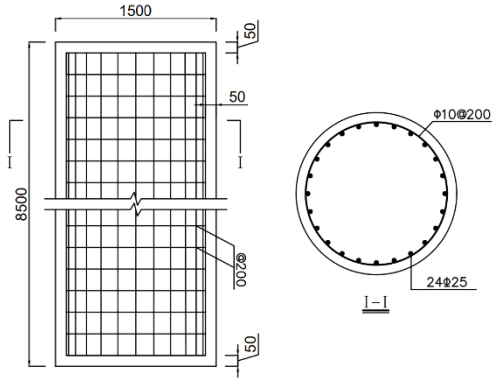


**Figure 1.** Pier size and reinforcement diagram (Unit: mm)

The pier reinforcement adopts three-dimensional beam element (Beam161) and concrete adopts three-dimensional solid element (Solid164). The grid of the area affected by the pier is refined. The size of the element is set to 0.05m, and the other parts are 0.1m. The finite element model of the pier is divided into 71832 elements. Concrete adopts HJC material model, which is widely used to describe large deformation and high strain rate conditions such as shock and explosion, and its yield surface equation is as follows:

$$\sigma^* = [A(1-D) + BP^{*N}](1 + C\ln\dot{\varepsilon}^*) \tag{1}$$

Where, $\sigma^*$, $P^*$ and $\dot{\varepsilon}^*$ are the ratio of actual effective stress to static yield strength, dimensionless pressure and dimensionless strain rate, respectively.

ISSN: 2414-1895 DOI: 10.6919/ICJE.202303_9(3).0008

For the specific meanings of other parameters of the model, refer to literature [9-10], and the parameter values are shown in Table 1.

**Table 1**. HJC concrete material parameters

| Input parameter | Magnitude | Input parameter | Magnitude |
|---|---|---|---|
| $\rho$(kg/m$^3$) | 2500 | $SF_{MAX}$ | 7 |
| $G$(Pa) | $1.35\times10^{10}$ | $P_C$(Pa) | $1.33\times10^{7}$ |
| $A$ | 0.79 | $U_C$ | 0.00071 |
| $B$ | 1.6 | $P_L$(Pa) | $8\times10^{8}$ |
| $C$ | 0.007 | $U_L$ | 0.072 |
| $N$ | 0.61 | $D_1$ | 0.0378 |
| $F_C$(Pa) | $4\times10^{7}$ | $D_2$ | 1 |
| $T$(Pa) | $3.92\times10^{6}$ | $K_1$(Pa) | $8.5\times10^{10}$ |
| $EPSO$ | 1 | $K_2$ (Pa) | $-1.7\times10^{11}$ |
| $EF_{MIN}$ | 0.01 | $K_3$ (Pa) | $2.08\times10^{11}$ |

The plastic follow-up strengthening model can describe the nonlinear deformation properties of reinforcement. The Cowper-Symonds model is adopted to consider the influence of strain rate effect, and its yield function [11] is:

$$\sigma=\left[1+\left(\frac{\dot{\varepsilon}}{C}\right)^{\frac{1}{P}}\right]\left(\sigma_0+\beta E_{\mathrm{p}}\varepsilon_{\mathrm{eff}}^{\mathrm{p}}\right) \tag{2}$$

Where, $\sigma$, $\dot{\varepsilon}$, $\sigma_0$, and $\varepsilon_{\mathrm{eff}}^{\mathrm{p}}$ are the yield stress, the material strain rate, the initial yield stress and the effective plastic strain of the material. $E_{\mathrm{p}}$ is the plastic hardening modulus of the material, and $E_{\mathrm{p}}=EE_{\mathrm{t}}/\left(E-E_{\mathrm{t}}\right)$. $C$ and $P$ are Cowper-Symonds strain rate parameters. For Marine mild steel, the values of $C$ and $P$ are 40.4 and 5, respectively. $\beta$ is the parameter for adjusting isotropic hardening and follow-up hardening. $\beta=1$ is isotropic hardening and $\beta=0$ is follow-up hardening. The concrete material parameters of reinforcement are shown in Table 2.

**Table 2**. Material parameters of reinforcement

| Input parameter | Mass density $\rho$(kg/m$^3$) | Young's modulus $E$(Pa) | Poisson's ratio $v$ | Yield stress $\sigma_0$(Pa) | Tangent modulus $G$(Pa) | Failure strain | C | P |
|---|---|---|---|---|---|---|---|---|
| Longitudinal reinforcement | 7800 | $2.1\times10^{11}$ | 0.3 | $3.35\times10^{8}$ | $1.18\times10^{9}$ | 0.35 | 40.4 | 5 |
| Stirrup | 7800 | $2.1\times10^{11}$ | 0.3 | $2.35\times10^{8}$ | $1.18\times10^{9}$ | 0.35 | 40.4 | 5 |

## 2.2 Vehicle Model

In this paper, Q235 steel mass blocks are used to simulate the vehicle, and the impact of vehicle deformation on the collision process is ignored. Therefore, the material model of the vehicle adopts the rigid body model. Specific parameters are shown in Table 3. The length, width and height of the rigid mass block are 3m×1.5m×0.4m. Three-dimensional solid element (Solid164) is adopted, and the grid of the head area is refined. The size of the element is set to 0.05m, and the other parts are 0.1m. The vehicle finite element model is divided into 8400 elements.

ISSN: 2414-1895 DOI: 10.6919/ICJE.202303_9(3).0008

**Table 3**. Material parameters of vehicle

| Input parameter | Mass density $\rho$(kg/m$^3$) | Young's modulus $E$(Pa) | Poisson's ratio $v$ |
|---|---|---|---|
| Stirrup | 1000 | $2.1\times10^{11}$ | 0.3 |

## 2.3 Aluminum Foam Collision Avoidance Device Model

The aluminum foam anti-collision device is arranged around the pier with a thickness of 0.2m and a three-dimensional solid element (Solid164) with a unit size of 0.04m. The anti-collision device is divided into 13,580 elements. MAT_CRUSHABLE_FOAM is used to simulate the aluminum foam material, whose constitutive relationship requires the stress-strain curve of the material, as shown in Figure 2. The detailed material parameters obtained from the test of aluminum foam by Wang Yonggang et al. [12] are shown in Table 4.

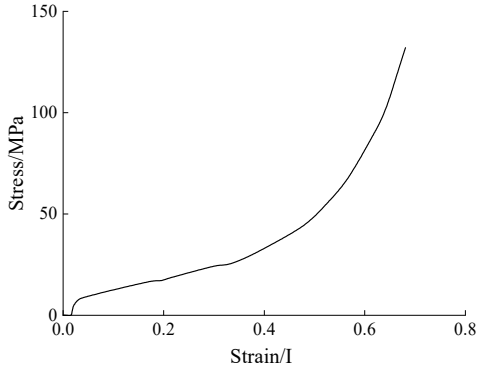


**Figure 2.** The stress-strain curve of aluminum foam

**Table 4**. Material parameters of aluminum foam

| Input parameter | Mass density $\rho$(kg/m$^3$) | Young's modulus $E$(Pa) | Poisson's ratio $v$ | Tensile stress cutoff $p_{cut}$(Pa) |
|---|---|---|---|---|
| Stirrup | 1200 | $2.1\times10^{9}$ | 0.3 | $1\times10^{7}$ |

## 2.4 Model of Vehicle Impact Pier

The vehicle impact speed is 60km/h and the impact height is 0.65m. The vehicle hits the center of the pier forward along the driving direction (X-axis), as shown in Figure 3. The pier bottom is constrained by the fixed end, and the freedom of 6 directions of the pier bottom node is set to zero. The pier top is the free end. The contact between vehicle and pier, vehicle and anti-collision device, and anti-collision device and pier adopts automatic face-surface contact, and the dynamic and static friction coefficients of contact surface are 0.3.

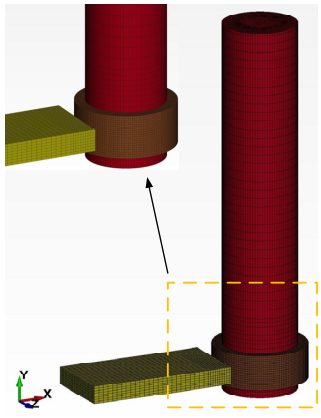

**Figure 3.** Model of vehicle impact pier

ISSN: 2414-1895 DOI: 10.6919/ICJE.202303_9(3).0008

## 3. Collision Result Analysis

The finite element model of vehicle-pier impact was established by ANSYS/LS-DYNA. The vehicle mass block was set to weigh 1.8t, and the vehicle was set to impact the bare pier and the pier with aluminum foam anti-collision device at the speed of 60km/h. The impact center height was 0.65m. The dynamic response characteristics of the piers with and without aluminum foam anti-collision devices were calculated and analyzed to study the protection effect of anti-collision devices on vehicles and piers.

### 3.1 Energy Analysis

Figure 4 shows the time history curve of energy change when vehicle impact bare pier. The total energy of the system is mainly composed of the following parts: kinetic energy, pier internal energy, hourglass energy and sliding energy. Before the collision, the kinetic energy of the vehicle is about 250000J, accounting for 100% of the total energy. After the collision, the kinetic energy of the vehicle is mainly transformed into the deformation energy of the pier, namely the internal energy. The internal energy accounts for 86.8% of the total energy. The residual kinetic energy of the vehicle accounts for about 6.96%. The slip energy is about 0.2%. Hourglass energy accounts for about 5.96%. The collision process basically follows the law of conservation of energy.

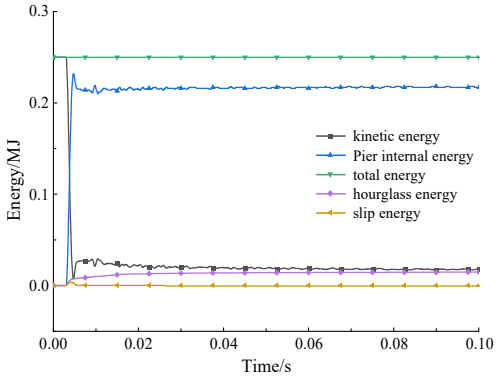


**Figure 4.** Time history curve of energy (without collision-prevention device)

Figure 5 shows the time history curve of energy change when a vehicle impinges on a pier with an anti-collision device. The total energy of the system mainly consists of the following parts: kinetic energy, internal energy of the anti-collision device, internal energy of the pier, hourglass energy and sliding energy. When there is an anti-collision device, during the collision process, the aluminum foam anti-collision device absorbs most of the kinetic energy of the vehicle through its own elastic and plastic deformation, accounting for 86.69%, while the energy absorbed by the pier only accounts for about 4%. The residual kinetic energy of the vehicle accounts for about 2.92%. Slip energy accounts for about 2%. The hourglass is about 4.8%. The collision process basically follows the law of conservation of energy.

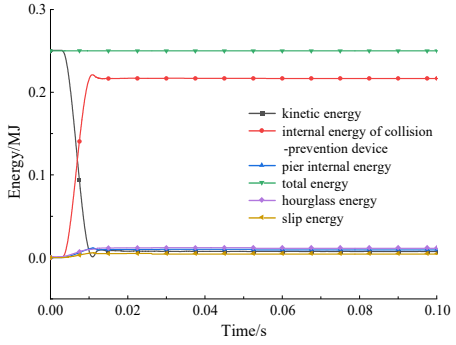


**Figure 5.** Time history curve of energy (with collision-prevention device)

ISSN: 2414-1895 DOI: 10.6919/ICJE.202303_9(3).0008

The sum of the hourglass energy and slip energy in the above two cases does not exceed 10% of the total energy, indicating that the hourglass energy and interface slip energy meet the control conditions, and the calculation results meet the requirements of finite element simulation [13], which verifies the rationality of the finite element model in the above two cases.

### 3.2 Impact Force Analysis

Figure 6 shows the time-history curve of the impact force when vehicles hit piers without and with anti-collision devices. In the process of collision, the time-history curve of the impact force presents obvious nonlinear characteristics. Due to the large stiffness of both the vehicle and the pier, the impact force immediately increases and reaches a peak after the collision, and then decreases rapidly with the separation of the vehicle from the pier or the anti-collision device. When there is no anti-collision device, the collision duration is 0.00255s and the peak impact force is 22.07MN. With the anti-collision device, the collision duration increases to 0.01095s and the peak impact force decreases to 6MN due to the good deformation energy absorption effect of the anti-collision device with aluminum foam. After the installation of aluminum foam anti-collision device, the peak value of impact force is reduced significantly, which is about 72.8% less than that without anti-collision device. The installation of aluminum foam anti-collision device can increase the impact duration, significantly reduce the impact force, and reduce the damage of vehicles and piers.

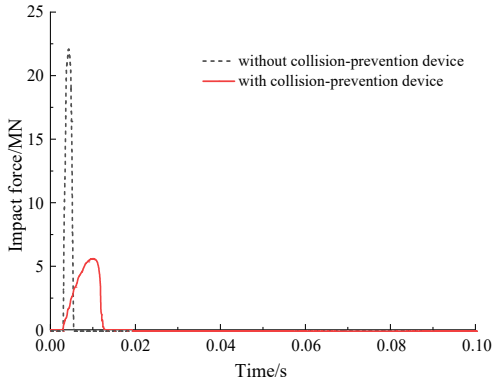


**Figure 6.** Time history curve of impact force

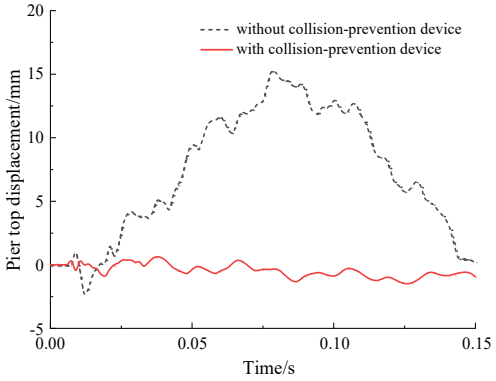


**Figure 7.** Displacement time history curve of pier top

### 3.3 Pier Displacement Analysis

The displacement response of the top of the tower is a key index to evaluate whether the bridge tower is safe. Figure 7 shows the time-history curve of the displacement of the top of the pier with or without the anti-collision device. The time-history curve of the displacement of the top of the pier presents obvious nonlinear fluctuation characteristics. When there is no anti-collision device, the impact force reaches the peak value at 0.00435s, and the maximum value of pier top displacement reaches 15.2mm at 0.078s. The maximum value of pier top displacement lags behind the peak value of impact force. With the anti-collision device, the maximum displacement of pier top is about 1.5mm, which is about

ISSN: 2414-1895 DOI: 10.6919/ICJE.202303_9(3).0008

90.13% less than that without the anti-collision device. The installation of foam aluminum anti-collision device can obviously reduce the displacement of pier top and enhance the security of pier.

### 3.4 Pier Stress Analysis

The stress time history curve of the impact surface of the bridge pier and the effective stress cloud diagram on impact surface at the moment of the maximum stress are shown in Figure 8 and Figure 9 respectively. The stress variation trend of the bridge pier can be judged by the time history curve of effective stress. When the collision occurs, the stress on the impact surface of the pier increases instantaneously. Due to the large kinetic energy of the vehicle, there is residual stress on the impact surface of the pier after the collision. The stress of the impact surface reaches its maximum in the center of the impact area and decreases gradually around it. Due to the constraint of fixed end at the bottom of the pier, the bending moment and shear force at the bottom of the pier are also large when it is impacted. When there is no anti-collision device, due to the small contact area between the vehicle and the pier, the peak stress on the impact surface of the pier is 200.6MPa, and part of the concrete is crushed. When there is an anti-collision device, due to the buffering effect of the anti-collision device, the peak stress of the impact surface of the pier is 39.12MPa, and the concrete of the pier is not damaged, which is reduced by 80.5% compared with that without the anti-collision device. After installing the foam aluminum anti-collision device, the stress on the collision surface of the pier can be reduced obviously, and the damage of the pier can be reduced.

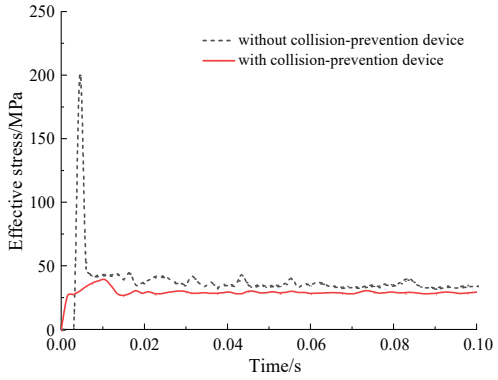


**Figure 8.** Time history curve of stress on impact surface

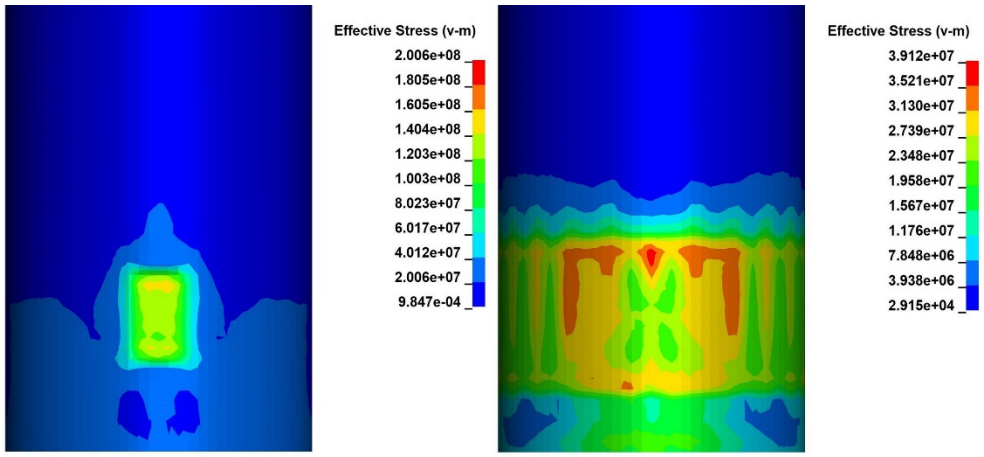


**Figure 9.** Effective stress cloud diagram on impact surface

### 3.5 Vehicle Acceleration Analysis

In order to simplify the study, the rigid body model was used in the finite element simulation of the vehicle in this paper, which did not consider the internal energy consumed by the deformation damage of the vehicle. However, the acceleration time history curve of the vehicle in the collision process plays an important role in judging the damage degree of the bridge and vehicle. FIG. 10 shows the

ISSN: 2414-1895 DOI: 10.6919/ICJE.202303_9(3).0008

time history curve of vehicle acceleration. When there is no anti-collision device, the maximum acceleration of the vehicle is about 6.98×103m·s-2. With the anti-collision device, the maximum acceleration of the vehicle is about 2.96×103m·s-2, which is 57.59% lower than that without the anti-collision device. The installation of foam aluminum anti-collision device can significantly reduce vehicle acceleration and reduce the damage of vehicles and piers.

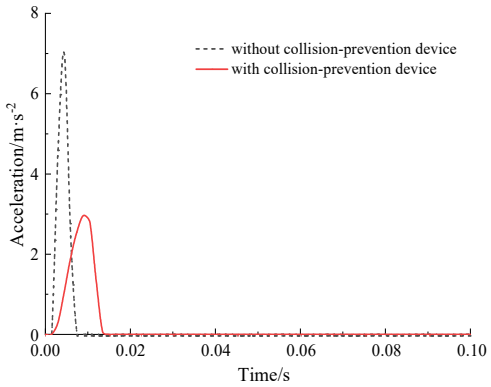


**Figure 10.** Acceleration time history curve of vehicle

## 4. Conclusion

The dynamic characteristics of the bridge pier with and without foamed aluminum were analyzed by finite element numerical simulation. The anti-collision effect of aluminum foam anti-collision device is compared and analyzed, and the following conclusions are drawn:

(1) The dynamic response of the pier can be effectively reduced after the installation of 0.2m thick aluminum foam anti-collision device. Compared with without the anti-collision device, the peak value of impact force decreases by 72.8%, the maximum value of pier top displacement decreases by 90.13%, the peak value of pier impact surface stress decreases by 80.5%, the maximum value of vehicle acceleration decreases by 57.59%, and the anti-collision device absorbed 86.69% of vehicle kinetic energy.

(2) The aluminum foam anti-collision device can absorb most of the kinetic energy of the vehicle through elastic and plastic deformation. After the installation of the aluminum foam anti-collision device, the vehicle acceleration can be reduced. The impact contact time can be increased. The impact force, pier top displacement, and pier impact surface stress can be reduced, effectively protecting the vehicle and pier.

## References

[1] F.Z. Dong, J. Guo, J.J. Wang. Summary of Bridge Collapse Accident and its Prevention Measures, Shanghai Highway, Vol. 2 (2009) No. 10, p. 30-32+38+13.

[2] J.K. Paik. Practical Techniques for Finite Element Modelling to Simulate Structural Crashworthiness in Ship Collisions and Grounding (Part II: Verification), Ships and Offshore Structures, Vol. 2 (2010), p. 81-85.

[3] M.H. Pradeep, Z.G Dhafer, C.D. Kan. Validation of a Single Unit Truck model for roadside hardware impact, Int. J. of Vehicle Systems Modelling and Testing, Vol. 2 (2007) No. 1, p. 1-15.

[4] G.C. Kantrales, G.R. Consolazio, D Wagner, et al. Experimental and Analytical Study of High-Level Barge Deformation for Barge-Bridge Collision Design, Journal of Bridge Engineering, Vol. 21 (2016) No. 2, p. 1-10.

[5] X.G. Zeng, W.J. Zhu, G.W. Tang, et al. Numerical Analysis of Dynamic Response and Impact Force of Pier under Vehicle Impact, Advanced Engineering Sciences, Vol. 2 (2012) No. 44, p. 171-174.

[6] Y. Han, D.Z. Fan, S. Liu. Experimental Study on the Influence of Outer Steel Plate on the Impact Performance of Reinforced Concrete Pier, Journal of Vibration and Shock, Vol. 23 (2017) No. 36, p. 175-180.

ISSN: 2414-1895 DOI: 10.6919/ICJE.202303_9(3).0008

[7] J.J. Wang, L.F. Tu, Y.G. Yin, et al. A Method for Designing Steel Plate-rubber Energy Absorption Ring, Vol. 2 (2019) No. 36, p. 50-60.

[8] Z.L. Wu, X.X Xu, L. Liu, et al. Research on Pavement Performance of Superpave Asphalt Mixture, Transportation Science & Technology, Vol. 4 (2008) No. 25, p. 74-77.

[9] T.J. Holmquist, G.R. Johnson, W.H. Cook. A Computational Constitutive Model for Concrete Subjected to Large Strains, High Strain Rates, and High Pressures, Proc.14th International Symposium on Ballistics, (1993), P. 591-600.

[10] F.G. Zhang, E.Z. Li. Determination Method of Concrete Impact Damage Model Parameters, Journal of Ballistics, Vol. 1 (2001) No. 4, p. 12-16+23.

[11] Y.C. Song, J.J. Wang, H.J. Yin, et al. Simplified Load Model of Ship-pier Collision, Journal of Vibration and Shock, Vol. 38 (2019) No. 5, p. 60-70.

[12] Y.G. Wang, SH.S. Hu, L.L. Wang. Experimental and Numerical Simulation of Shock Wave Attenuation in Aluminum Foam under Explosion Load, Explosion and Shock Waves, Vol. 6 (2003) No. 6, p. 516-522.

[13] R.X. Hu, S.T. Kang. ANSYS 18.0/LS-DYNA Nonlinear Finite Element Analysis Example Guide Tutorial (China Machine Press, China 2018), p. 27. (In Chinese).